A Method to Help Identify the Source of Epileptic Seizures

Applying Time-Frequency Analysis to Seizure EEG Activity

S. Blanco[1], S. Kochen[2], O.A. Rosso[1], and P. Salgado[2]
[1]Instituto de Calculo, FCEyN, Universidad de Buenos Aires, Pabellon II, Ciudad Universitaria; [2]Centro Municipal de Epilepsia, Division Neurologia, Hospital Ramos Mejia, Universidad de Buenos Aires

Defining the precise anatomical origin of ictal electrical discharges is necessary to decide the limits of a therapeutic surgical intervention in patients with severe, drug-resistant partial epilepsies. In general, the epileptogenic zone is inferred from visual analysis of electroencephalographic (EEG) ictal and interictal activity, together with the clinical patient history. These EEG signals can be obtained with stereotactic techniques, which aim to measure the electrical activity of the brain in three dimensions. Thus, methods for analysis of ictal recording that assist in seizure localization can be valuable tools in pre-operative evaluation of patients with refractory partial seizures. Analysis of EEG signals always involves the queries of quantification, i.e., the ability to state objective data in numerical and/or graphical form. Without such measures, EEG appraisal remains subjective and can hardly lead to logical systematization [1-5].

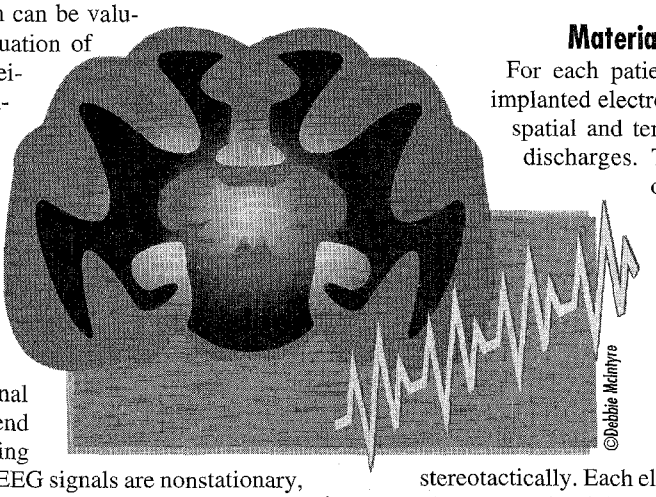

The EEG is a complex signal whose statistical properties depend on both space and time. Regarding the temporal characteristics, the EEG signals are nonstationary, and from the dynamical point of view, they are chaotic. Nevertheless, they can be analytically subdivided into representative epochs [1-6]. The most popular way of performing frequency analysis has been to apply the fast Fourier transform (FFT) algorithm directly to a short, usually 1-4 sec, segment of digitized data and average over the partial spectra of the complete signal [1-5]. The FFT method assumes, however, that the signal is stationary and is insensitive to its varying features.

In this article, we apply the method based on the Gabor transform (GT) for the simultaneous treatment in the time-frequency space of EEG signals [7]. This method allows us to analyze the time evolution of the traditional frequency rhythm of an EEG signal and visualize the frequency-band behavior during epileptic seizure. The linear correlation between the obtained frequency evolution series (for the different channels and frequency bands) can be used to obtain information about the interaction and, consequently, the causality between EEG signals from different regions of the brain and the frequency bands in other regions. The systematic calculation of these correlations, together with the clinical patient history and the visual assessment of the EEG, can be a valuable tool for the identification of the epileptic focus, as well as for the study of seizure dynamics.

Material and Methods

For each patient, the strategy for the use of implanted electrodes is planned in relation to the spatial and temporal organization of the ictal discharges. This information is simultaneously correlated with clinical symptomatology.

Here we present a patient's study selected because he presents a different seizure activity from a previous paper [7]. The patient whose analysis is shown here was explored with 8 multilead depth electrodes of 1 mm thickness implanted stereotactically. Each electrode carried 10 or 15 cylindrical contacts of a nickel-chromium alloy with a length of 2 mm and intercontact distance of 1.5 mm. In Fig. 1, we display a schematic diagram of the position and notation of the electrodes.

Each signal was amplified and filtered using a 1-40 Hz band-pass filter. A 4-pole Butterworth filter was used as a low-pass filter for anti-aliasing. After 10 bits A/D conversion, the EEG data were written continuously onto a disk of a data acquisition computer system with a sampling rate of 256 Hz per channel. Selected artifact-free EEG data sets of ictal and interictal activity were stored for subsequent off-line analysis.

According to the visual assessment of the EEG seizure recording, this patient presented an epileptogenic area in the left amygdala with immediate propagation to the left hypocampus and then to the right contralateral homologous area. In Fig. 2,

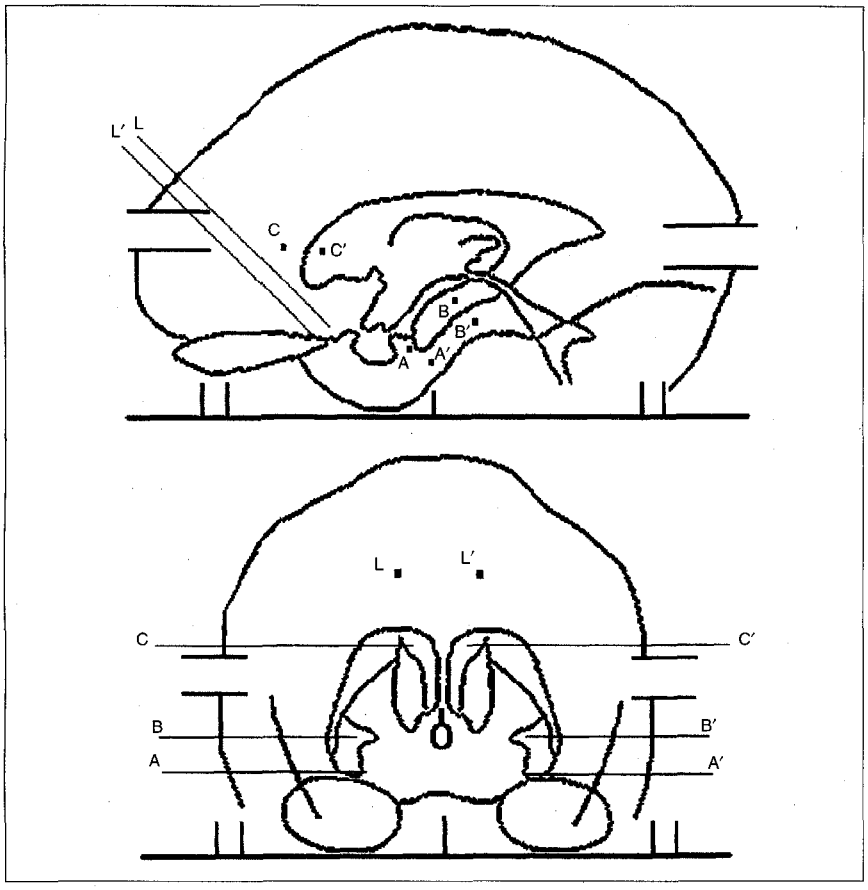

1. Schematic location of depth electrodes. Abbreviations: A(A′) Right (Left) Amygdalin Nucleus (10 contacts); B(B′) Right (Left) Hypocampus (10 contacts); C(C′) Right (Left) Gyrus Cingular (15 contacts); L(L′) Right (Left) Frontal Lobe (15 contacts).

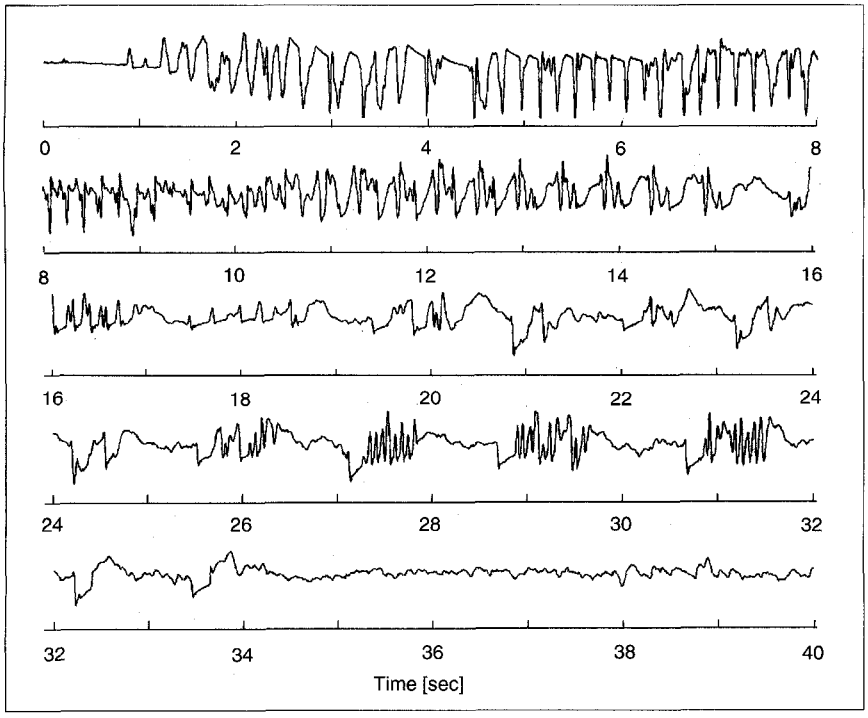

2. Recording of the EEG signal corresponding to a contact in the epileptogenic region, left amygdala (A'_3).

as an example, we display the EEG signal for 40 sec corresponding to the contact in the left amygdala (A'_3) nearest to the epileptic focus. This sample was displayed in such a way that the epileptic seizure starts around the 0 second and finishes around the 34th second.

Time-Frequency Analysis

In the traditional analysis of the EEG series [1-5], the frequency-time evolution was not taken into account or, as in the case of compressed spectra, it only provided a difficult-to-interpret visualization. In summary, traditional spectral analysis only quantified the amount of activity in frequency bands, though important information about peak timing was lost.

In a previous work [7], we introduced a time-frequency analysis that takes the GT [8] as a basic element. The GT is similar to the FFT, but with the advantage that it allows the analysis of the frequencies and their time evolution. The GT is equivalent to a wavelet algorithm with a fixed window [9]; but we employed the GT due to the following: a) in the analyzed frequency range, both methods are equivalent using an appropriate window, and b) the GT is easily comprehensible by its analogy with the FFT.

From a practical point of view, the GT can be thought of as an FFT with a temporal window over short epochs. This window slides along the entire signal, thereby providing information on the frequency changes with time. The EEG signal and its variation with time can be denoted as $X(t)$. After the GT, this signal is defined at ω_o and time t_o, similar to the FFT by:

$$G_D(\omega_o, t_o) = \int_{-\infty}^{\infty} X(t) g_D^*(t - t_o) e^{i\omega_o t} dt \quad (1)$$

where G_D (ω, t) symbolizes the GT, ω represents the frequencies, and t represents the time. The parenthesis notation indicates that GT varies with frequency and time. The subscript D is used to denote the length of the epoch under consideration. $gD(t - t_o)$ represents the temporal window being considered, i.e., having a width D and localized temporarily in t_o. We worked with a Gaussian window as suggested by Gabor. In this way, the introduction of false frequencies is avoided when performing the GT. This Gaussian window is recommended for the time-frequency analysis in order to achieve maximal concentration in time and frequency.

In our case, the window was set as D =

4 sec (2048 data). If we take $g_D = 1$, that is, without considering this window, the previous equation is the traditional definition of the Fourier transform of the signal $X(t)$. In the present analysis, the slide Gaussian window is displaced 64 data points, which is equivalent to make a GT each 0.25 sec of signal. Thus, the resolution in the time-frequency space was: $\Delta\omega = 0.125$ Hz, and $\Delta t = 0.25$ sec.

The next step is based on the following definitions. We defined the time evolution of the *spectral frequency content*, and we denoted by $\mathcal{B}^{(i)}$, for the band i (i = δ, θ, α, β_1, β_2) as:

$$\mathcal{B}^{(i)}(\omega,t) = \left|\mathcal{G}_D(\omega,t)\right|^2$$
$$\forall \omega^{(i)}_{\min} \le \omega \le \omega^{(i)}_{\max} \qquad (2)$$

This quantity is defined in the frequency interval ($\omega^{(i)}_{\min}$, $\omega^{(i)}_{\max}$). Here, $\omega^{(i)}_{\min}$ and $\omega^{(i)}_{\max}$ represent the minimum and maximum frequency values that define the i-band. The power spectral intensity for the i-band as a time function will be the sum of the spectral frequency content for each one of the frequencies included in the frequency interval ($\omega^{(i)}_{\min}$, $\omega^{(i)}_{\max}$). Then, for the i-band, the power spectral intensity as a function of time will be:

$$I^{(i)}(t) = \sum_{\omega=\omega^{(i)}_{\min}}^{\omega^{(i)}_{\max}} \mathcal{B}^{(i)}(\omega,t) \qquad (3)$$

Consequently, the total spectral power intensity ($I_T(t)$) is the sum of the intensities for all the bands considered. We also defined the power spectral intensity per band relative to the total intensity:

$$R^{(i)} = (I^{(i)} / I_T) \times 100 \qquad (4)$$

For the subsequent analysis of the EEG signal, we define for the different bands a kind of average frequency, *the mean weight frequency* value $\tilde{\omega}$ at time t, as:

$$\tilde{\omega}^{(i)}(t) = \left[\sum_{\omega=\omega^{(i)}_{\min}}^{\omega^{(i)}_{\max}} \omega \cdot \mathcal{B}^{(i)}(\omega,t)\right] / \left[\sum_{\omega=\omega^{(i)}_{\min}}^{\omega^{(i)}_{\max}} \mathcal{B}^{(i)}(\omega,t)\right] \qquad (5)$$

Note that if the spectral content is the same for all frequencies, the previous definition becomes the usual definition for mean value.

Finally, we defined the *main peak frequency* in the i-band at time t, $\omega^{(i)}_M$ as the frequency value for which $\mathcal{B}^{(i)}$ takes its

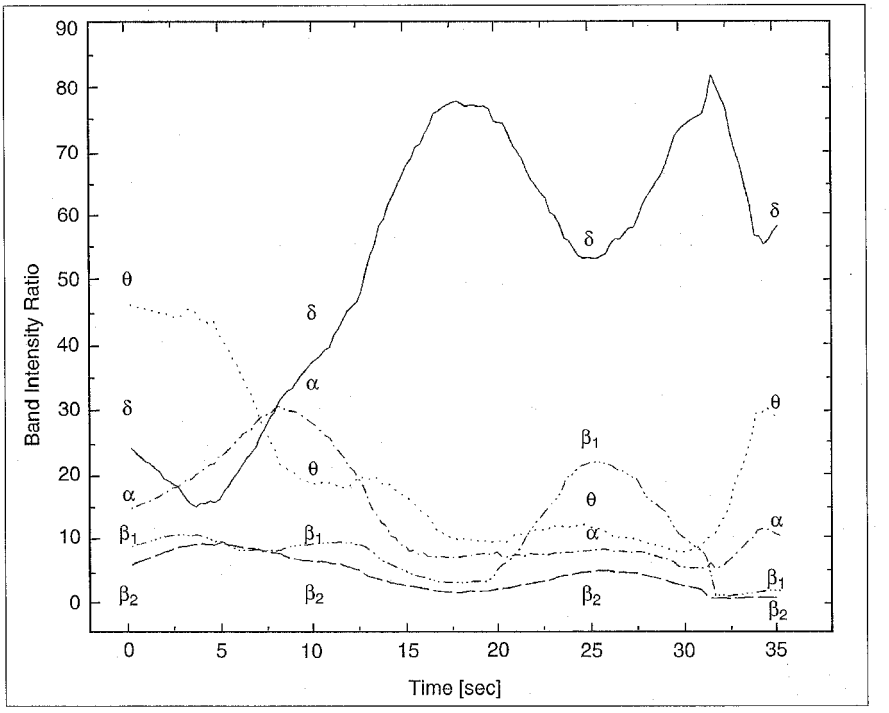

3. Power spectral intensity per band relative to the total intensity, as a function of time for the EEG signal showed in Fig. 1

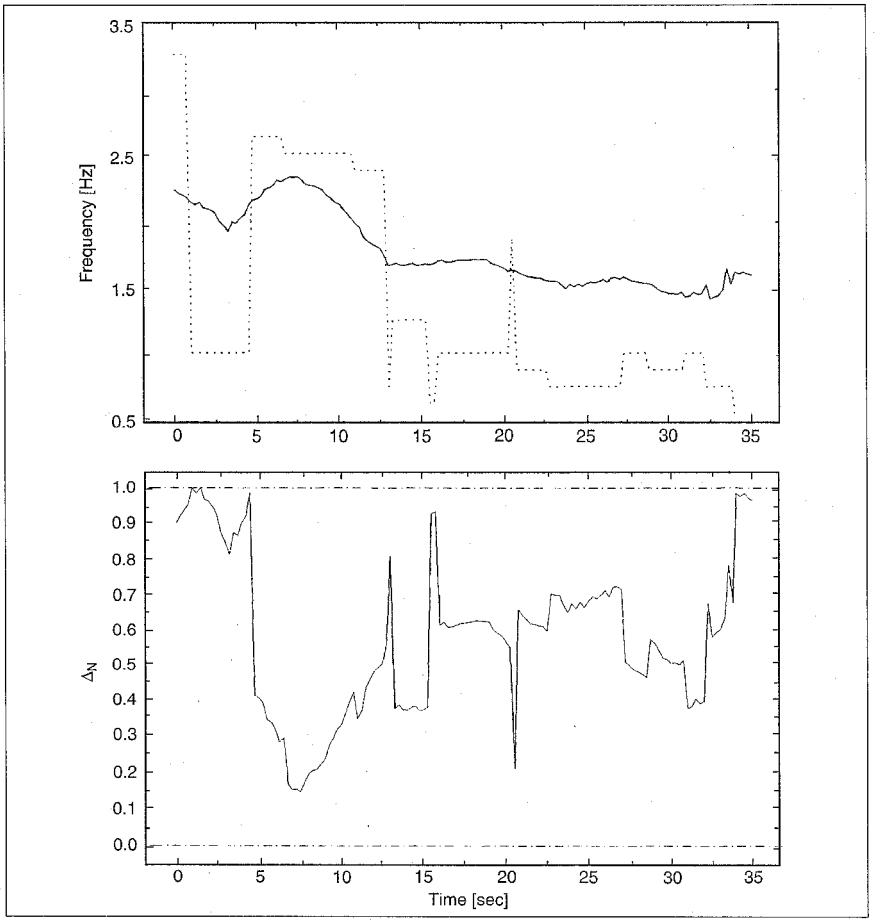

4. (a) Time evolution of the mean frequency $\tilde{\omega}$ (full line) and main peak frequency ω_M (dotted line) for delta band. (b) Normalized monofrequency deviation for delta band.

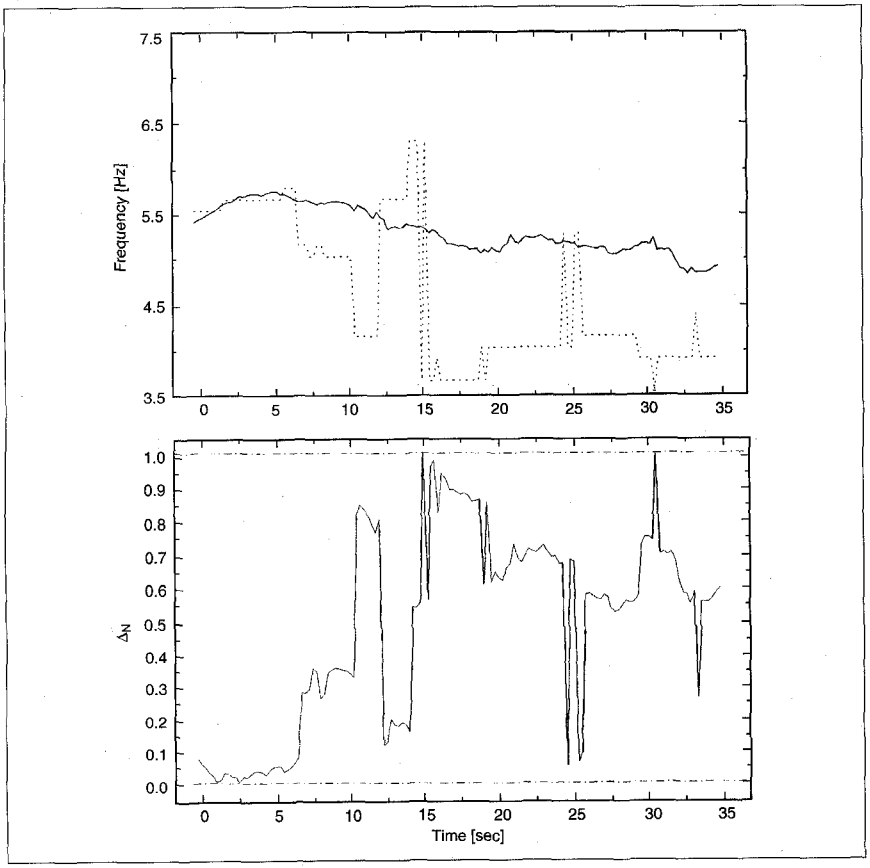

5. Same as Fig. 4 but for the theta band.

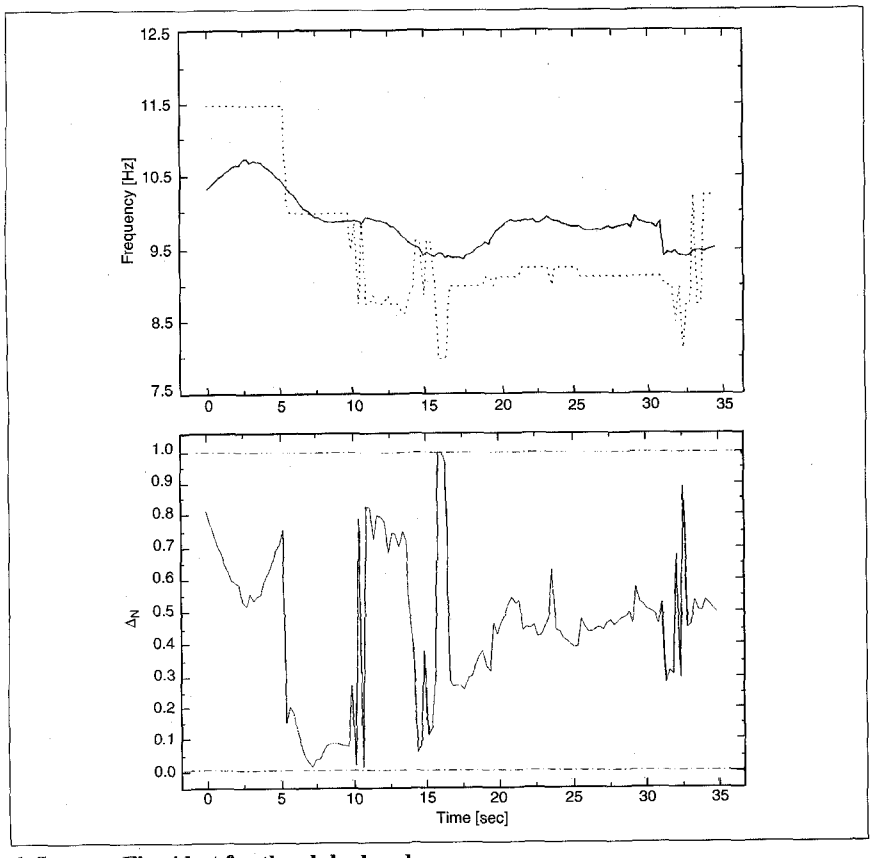

6. Same as Fig. 4 but for the alpha band.

maximum value in the interval ($\omega^{(i)}_{min}$, $\omega^{(i)}_{max}$):

$$\mathcal{B}^{(i)}(\omega_M, t) > \mathcal{B}^{(i)}(\omega, t)$$
$$\forall\ \omega \neq \omega_M \in (\omega^{(i)}_{min}, \omega^{(i)}_{max}) \qquad (6)$$

The Fourier spectrum will be represented by only one sharp peak at one frequency in presence of a monofrequency signal. For this case, if we evaluate the mean weight frequency and the main peak frequency, they will both be the same. Therefore, when $\tilde{\omega}(t)$ is approximately equal to $\omega_M(t)$ *during an appreciable time interval* in some band, we shall say that we are in the presence of a *quasi-monofrequency engagement* in that band. We stress that in our formalism, a signal will be quasi-monofrequent in a band if this engagement is observed during a *reasonable period* related with the total time-seizure duration. In our case, we considered that the minimum time in order to define this behavior is 2 sec, which represents about 5% of the seizure duration.

Now, we introduce a new parameter, $\Delta^{(i)}$, and call it *monofrequency deviation.* This parameter, as a function of time, gives us an idea about the periods in which the engagements are relevant:

$$\Delta^{(i)}(t) = \left|\tilde{\omega}^{(i)}(t) - \omega^{(i)}_M(t)\right| \qquad (7)$$

Moreover, in order to compare these new time series, for different bands and channels, we normalized each one to its maximum value ($\Delta^{(i)}_N(t) = \Delta^{(i)}(t) / \Delta^{(i)}_{max}$).

The importance of having introduced these new time series, $R(t)$, $\tilde{\omega}^{(i)}(t)$, $\omega^{(i)}_M(t)$ and $\Delta^{(i)}_N(t)$, is that they allow us to characterize the epileptic seizure as well as its evolution with time by means of quantifiable magnitudes that are independent of the signal's morphology.

Results and Discussion

In order to discuss this type of time-frequency analysis, we divided the signal shown in Fig. 2 into different time intervals. These intervals were suggested by the modifications of the signal pattern. By visual inspection, the intervals are: 0 to 1 sec - fast activity and decrease of amplitude; 1 to 2 sec - low and clonic activity with increasing amplitude; 2 to 5 sec - spike discharges embedded in slow activity; 5 to 9 sec - spikes and waves discharges with frequencies around 5-6 Hz; 9 to 11 sec - spikes with frequency around 9-10 Hz; 11 to 15 sec - polispike and wave

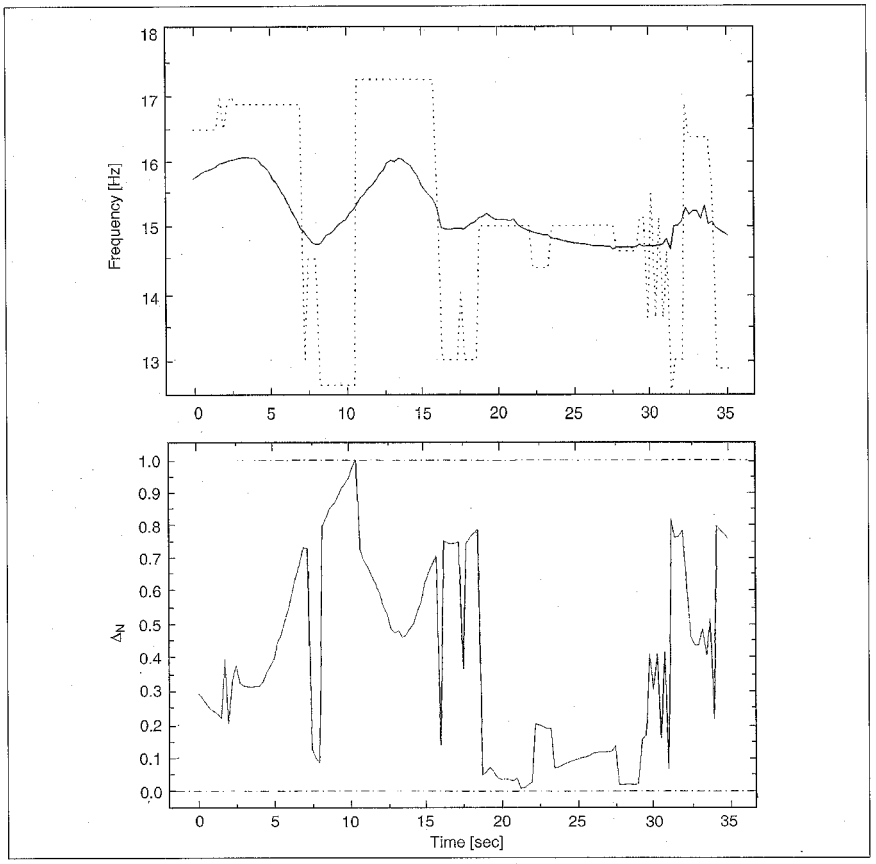

7. Same as Fig. 4 but for beta-1 band.

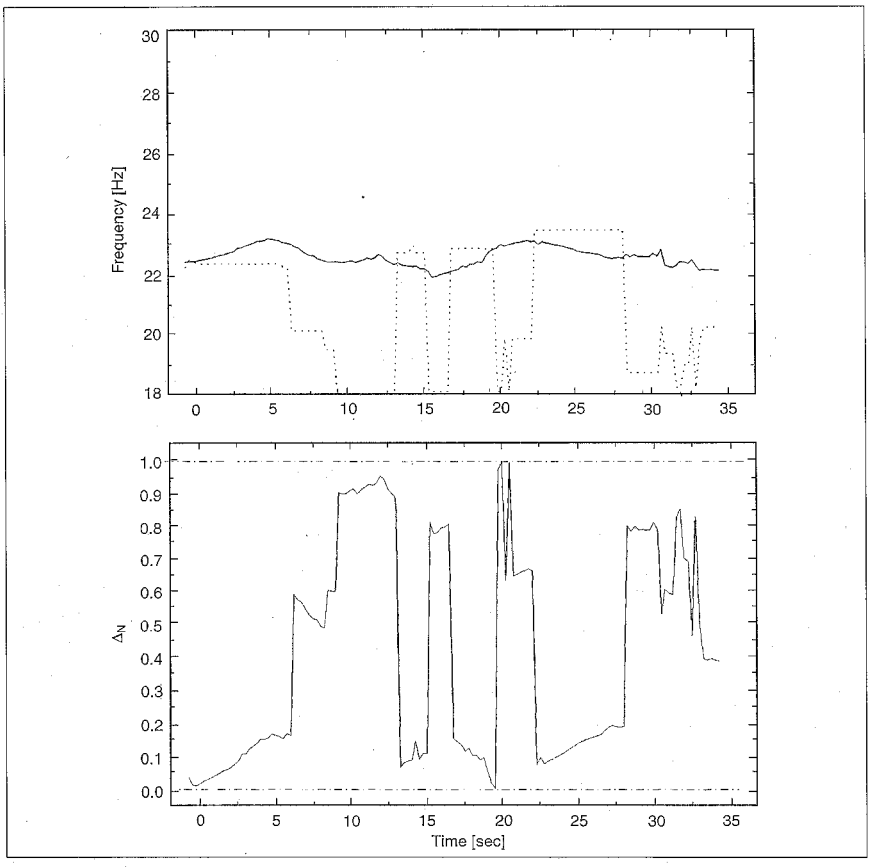

8. Same as Fig. 4 but for Beta-2 band.

complexes; 15 to 32 sec - very low activity with high-frequency discharges (burst).

In Fig. 3, we show the spectral intensity per band relative to the total intensity, $R^{(i)}$, as a function of time for the EEG signal shown in Fig 2. In Figs. 4 to 8, we display the time evolution of $\tilde{\omega}^{(i)}$ and ω_M for the different bands and $\Delta_N^{(i)}(t)$.

In these figures, we can see that when $\tilde{\omega} \sim \omega_M$ or, equivalently, when $\Delta_N^{(i)}(t) \sim 0$, a quasi-monofrequency band behavior has evolved. This can be understood as *a quasi-monofrequency engagement* if its duration is greater than 2 sec and its value is $\Delta_N \leq 0.2$.

We want to stress that these new time series provide quantifiable objective information about the frequency content and the relative intensities present in each interval of the EEG signal. In this way, hidden information can be put in evidence. For example, a fast activity, which is evident in a first visual inspection, could be modulated by a low frequency that is not easy to detect in the EEG trace. This kind of behavior can be observed at 11-14 sec in Fig. 2. The polispike and wave complex trains are modulated by a low-frequency wave in the delta band. This potentially hidden information can be better appreciated by analyzing Figs. 3-8 with the same intervals as chosen by the visual inspection.

0 to 1 sec: The seizure begins. There is a predominance in the theta rhythm followed by a contribution in the delta frequencies (Fig. 3). A starting engagement in the theta ($\Delta_N^{(\theta)} \sim 0$) and beta-2 bands ($\Delta_N^{(\beta_2)} \sim 0$), can be observed (Figs. 5 and 8).

1 to 5 sec: The predominance of the theta rhythm still continues with values similar to the previous interval. There is a decrease in the relative intensity of the delta rhythm, with a minimum value toward the end of the interval. There is an increase in the alpha frequencies (Fig. 3). There is still a strong engagement in the theta ($\Delta_N^{(\theta)} \sim 0$) and beta-2 ($\Delta_N^{(\beta_2)} < 0.15$) is fading away (Figs. 5 and 8).

5 to 9 sec: There is a noticeable decrease in the relative intensity of the theta rhythm, with an increment in the alpha activity with a maximum at the end of the interval. There is a marked increase in the delta band (Fig. 3). There seems to be a tendency toward a delta engagement ($\Delta_N^{(\delta)} \sim 0.2$) and a strong alpha ($\Delta_N^{(\alpha)} \sim 0.1$) engagement (Figs. 4 and 6).

9 to 12 sec: Delta intensity continues

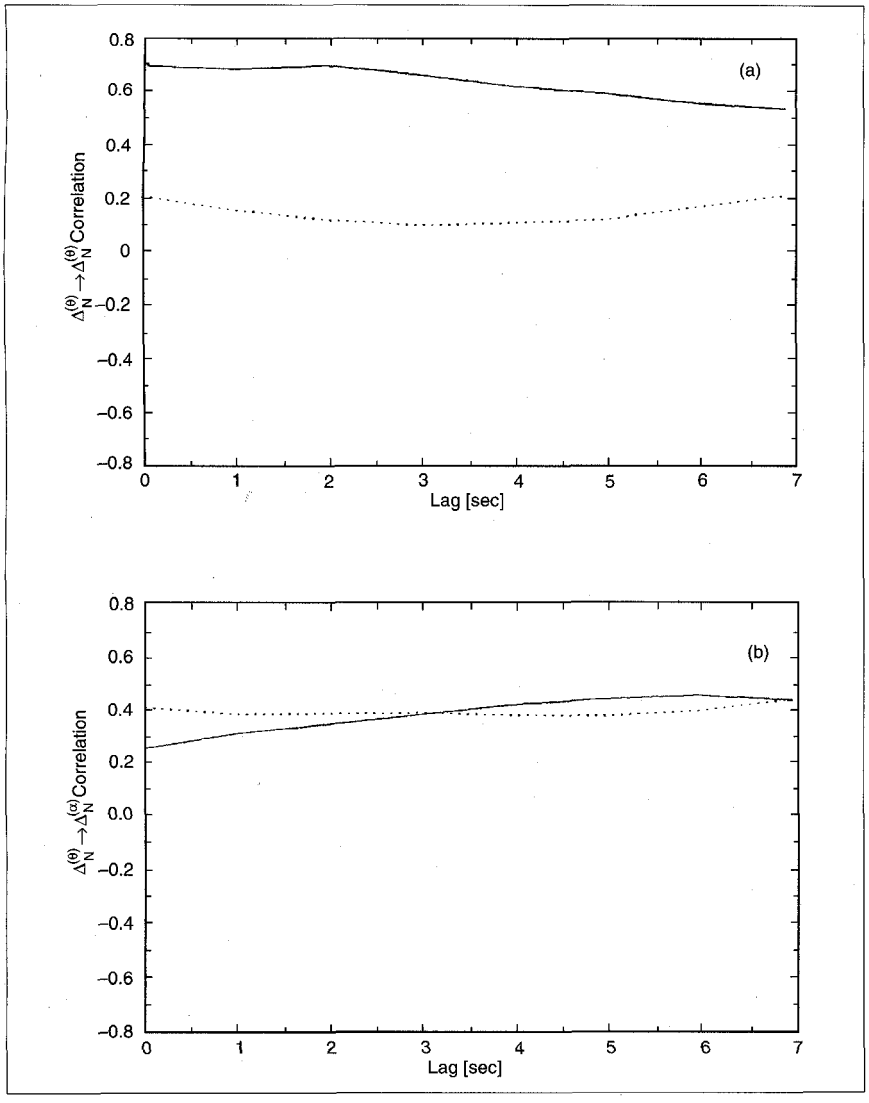

9. Lag correlation in units of Δt between monofrequency deviation time series between a contact in the epileptogenic region and contacts in the immediate propagation area. $A'_3 \rightarrow B'_4$ (dotted line). (a) theta-theta correlations; (b) theta-alpha correlations.

to grow and alpha starts to diminish (Fig. 3). The theta activity remains close to constant; intermittent alpha engagements are observed (Fig. 6).

12 to 15 sec: The delta activity becomes dominant while there is a clear decrease in alpha (Fig. 3). There is a tendency towards theta ($\Delta_N^{(\theta)} \sim 0.2$) and beta-2 ($\Delta_N^{(\beta_2)} \sim 0.1$) engagements in the first and second half of the interval, respectively (Figs. 5 and 8).

15 to 26 sec: The delta activity is predominant, with a maximum around 20 sec. The beta-1 activity shows an increase in its relative intensity from 20 sec onwards, with a maximum range at 25 sec, coinciding with a Delta minimum (Fig. 3). There is a tendency toward alpha engagement ($0.3 < \Delta_N^{(\alpha)} < 0.5$) with beta-1 ($\Delta_N^{(\beta_1)} < 0.2$) and beta-2 ($\Delta_N^{(\beta_2)} < 0.2$) engagements (Figs. 6, 7, and 8).

26 to 32 sec: Delta activity still remains dominant with an increment in its relative intensity (Fig. 3). Beta-1 decreases; a tendency for an alpha engagement persists ($\Delta_N^{(\alpha)} \sim 0.5$), intermittent beta-1 ($\Delta_N^{(\beta_1)} < 0.15$) and beta-2 ($\Delta_N^{(\beta_2)} < 0.2$) engagements are observed coinciding with paroxysmal bursts (Figs. 6, 7 and 8).

32 to 40 sec: End of the seizure. The delta rhythm predominates with a parallel increase in the theta relative intensity (Fig. 3). No quasi-monofrequency behaviors are observed.

To conclude, this seizure can be characterized to have a theta- and beta-2-dominant monofrequency at the beginning, which rapidly evolves to a dominant alpha monofrequency for the rest of the seizure.

The frequency engagements, prior to and during seizure, can be used as a method for detecting the *information transfer* between channels (brain zones), involved in the epileptogenic zone and the other zones of the brain. When we speak about "information transfer," we do not claim to explain the underlying neurophysiology evolved in the seizure propagation. We want to show how the dynamical behavior of the seizure in a band and in a determined channel of the epileptogenic zone affects the dynamical behavior in other bands in channels that are not so close.

The $\Delta_N^{(i)}$ parameter as a time function gives us an idea about the periods in which the engagements are relevant. It is interesting to note that we did not observe $\Delta_N^{(i)} \leq 0.2$ extended in time in the EEG background activity except for isolated paroxysms.

If we evaluate the linear correlation among the time series $\Delta_N^{(i)}$ arising from two different channels and corresponding bands as a function of a time shift, τ, we can investigate when an engagement in one channel and band induces a similar behavior in another channel and band. Then, the correlation will be large at some value of time lag, τ, if the first time series ($\Delta_N^{(i)}$) is a close copy of the second ($\Delta_N^{(j)}$) but lags in time by, τ; i.e., if the first time series is shifted to the right of the second. This time, τ, is a measure of the delay in which the dynamical behavior in a channel and band is copied by the other channel or band. Therefore, only the first seconds of the delay are the relevant.

From now on, we will analyze the theta-theta and theta-alpha correlations because the theta and alpha engagements were identified as the relevant ones in the seizure. In Figs. 9a-11a we display the lag correlation for τ between 0-7 Δt sec for the $\Delta_N^{(\theta)} \rightarrow \Delta_N^{(\theta)}$ and in Figs. 9b-11b we display the $\Delta_N^{(\theta)} \rightarrow \Delta_N^{(\alpha)}$ correlations.

Fig. 9 corresponds to the correlation between a contact where the seizure starts, left amygdala ($\mathbf{A}'_3$), and two signals provided by contacts located in left amygdala ($\mathbf{A}'_2$) and left hypocampus ($\mathbf{B}'_4$), that is, in the immediate propagation region. We observe in Fig. 9a a high correlation theta-

theta for $\mathbf{A'}_3 \rightarrow \mathbf{A'}_2$, with small decrease for lags greater than 2 sec. A small correlation value, almost constant for this lag time, is observed for $\mathbf{A'}_3 \rightarrow \mathbf{B'}_4$. The values for theta-alpha correlations are quite significant and almost constant for both signals (see Fig. 9b).

The correlation between the signal $\mathbf{A'}_3$ and the epileptogenic focus contralateral homologous region is presented in Fig. 10. The theta-theta correlation for $\mathbf{A'}_3 \rightarrow \mathbf{A}_3$ and $\mathbf{A'}_3 \rightarrow \mathbf{B}_2$, and the theta-alpha correlation for the same contacts are shown in Figs. 10a and 10b, respectively. We observe high theta-theta correlation, almost constant in time, for both contacts (Fig. 10a) and low correlation for the theta-alpha bands with the hypocampus contact (Fig. 10b).

For signals provided by contacts out of the immediate propagation region, frontal lobe (**L**), and gyrus cingular (**C**) we observed small correlation values for the theta-theta and theta-alpha bands, with decreasing values in some cases. This behavior is exemplified in Fig. 11 for $\mathbf{A'}_3 \rightarrow \mathbf{C}_2$ and $\mathbf{A'}_3 \rightarrow \mathbf{L}_2$.

Although the mathematical linear correlation was done among all frequency bands of all available signals (contacts), those which present a meaningful behavior were the bands with the strongest engagements. From these results, we can observe that an engagement in a band can induce engagements in another channel and in other bands, shedding light on a special characteristic of the seizure. Moreover, higher correlations are observed between signals in the epileptogenic region and the immediate propagation region (as was exemplified in Figs. 9-11), and a lesser correlation with decreasing values correspond to signals in the out-of-immediate seizure propagation region (Fig. 11). The behavior observed with these tools allows us to make the dynamic assumption that the epileptogenic zone (focus) acts as a global pacemaker with some characteristic frequency, determined by the frequency engagements.

Even though we only show a few correlations here, all of them have been evaluated. The agreement between the correlation behavior described above and the localization of the epileptic focus and the propagation areas was very good. Similar analyses were made for three different patients evaluated for surgical treatment, with high correlation between both points of view, that is, the physician local-

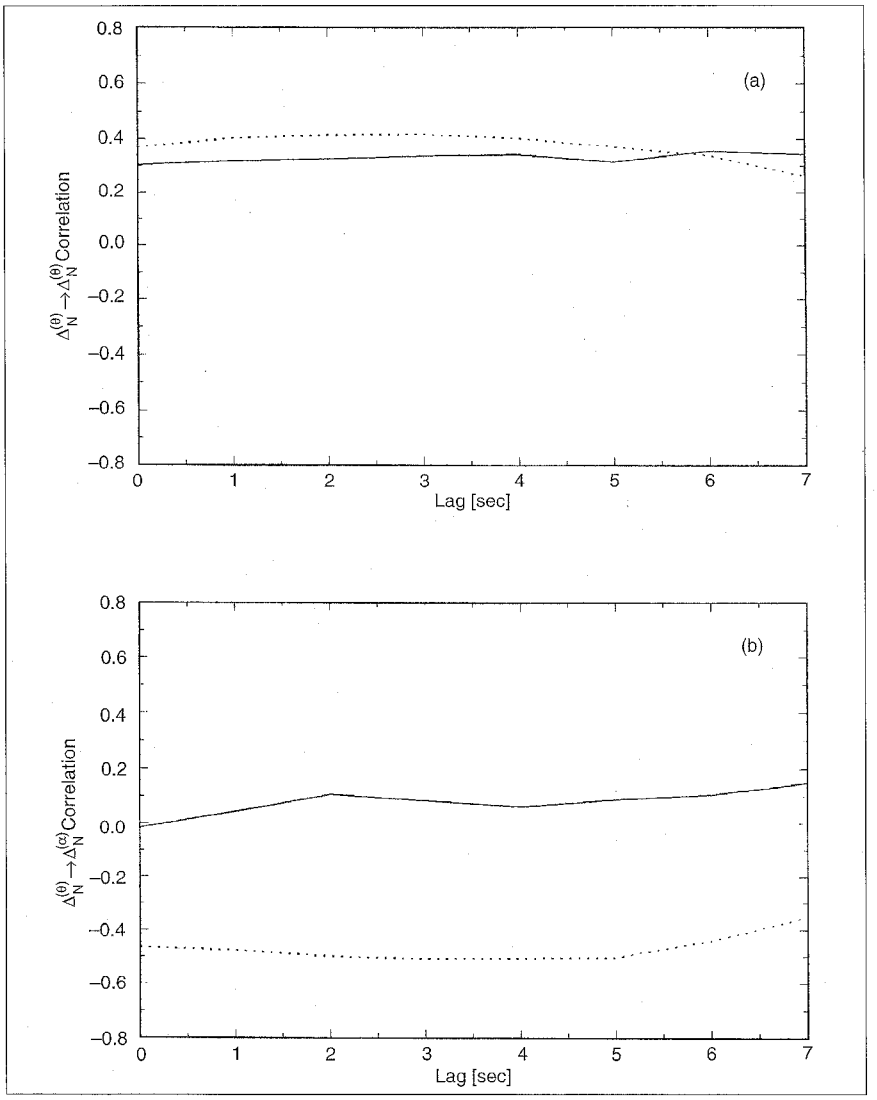

10. Lag correlation in units of Δt between monofrequency deviation time series between a contact in the epileptogenic region and contacts in the homologous contralateral propagation area. $\mathbf{A'}_3 \rightarrow \mathbf{A}_2$ (full line). $\mathbf{A'}_3 \rightarrow \mathbf{B}_2$ (dot line). (a) theta-theta correlations; (b) theta-alpha correlations.

ization and the engagements band correlation. Thus, this technique is a possible tool to distinguish contacts in one epileptogenic region from another region.

Conclusions

In this article we confirmed the previous results about the ability to perform an EEG time-frequency analysis in a systematic way. This method gives an accurate description of the time evolution of the rhythm defined in the epileptic activity. We can generate a time series that quantifies the dynamic behavior of brain activity, independent of the EEG signal morphology. In particular, the lag correlation among these new time series gives a good picture of the information transfer process of epileptiform activity throughout the brain.

We applied this method to intracranial EEG records of epileptic refractory patients. We conclude that the epileptic seizure could be characterized by a quasi-monofrequency activity for some of the bands. This characteristic can be used to analyze the epileptic seizure and to study the dynamic changes in its time evolution.

The use of the present time-frequency analysis, together with patient clinical history and the visual assessment of the EEG, can contribute to the identification of the source of epileptic seizure activity and of its propagation within the brain. Furthermore, it yields new insights with respect

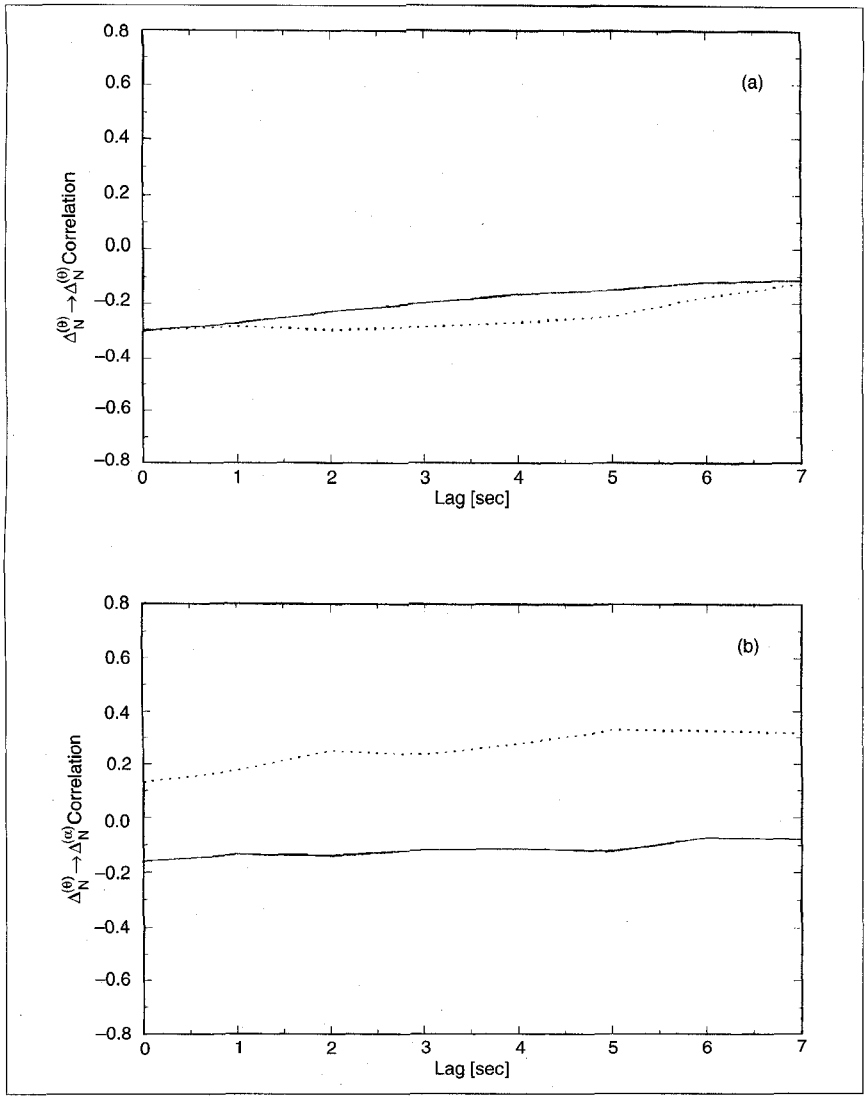

11. Lag correlation in units of Δt between monofrequency deviation time series between a contact in the epileptogenic region and contacts out of immediate propagation area. $A'_3 \rightarrow C_2$ (full line). $A'_3 \rightarrow L_2$ (dotted line). (a) theta-theta correlations; (b) theta-alpha correlations.

to the behavior of the electrical activity during the seizure.

Acknowledgments

This work was supported by the Consejo Nacional de Investigaciones Cientificas y Tecnicas (CONICET) and University of Buenos Aires, Argentina. Two of us (O.A.R. and S.B.) undertook this work with the support of Fundacón Alberto J. Roemmers (Argentina). The comments of two anonymous reviewers were responsible for a significant improvement in the manuscript. We are thankful to Dr. F.H. Lopes da Silva, Dr. J. P. N. Pijn, Lic. L. Riquelme and Lic. R. Quian Quiroga for stimulating and useful discussions.

Susana A. Blanco was born in Buenos Aires, Argentina, on January 17, 1952. She received the M.S. and Ph.D. degree in Physics from University of Buenos Aires, Argentina, in 1981 and 1989, respectively. Her research interests are in the field of nonlinear dynamical systems and their applications to biologycal and medical sciences.

Dr. Blanco is a member of the Scientific Research Center of the National Research Council (CONICET - Argentina) and Co-Head of the Master on Medical Physics (University of Buenos Aires).

Osvaldo A. Rosso was born in Rojas, Argentina, on October 15, 1954. He received the M.S. and Ph.D. degrees in Physics from the University of La Plata, Argentina, in 1978 and 1984, respectively. He held a post-doctoral position at Forschungzentrum Jülich GmbH (KFA), Jülich, Germany, from 1988 to 1990, and was a visiting researcher at Sezione di Cinematografia Scientifica (CNR), Bologna, Italy, from 1990 to 1992. His research interests are in the field of nonlinear dynamical systems and their applications to biological and medical sciences.

Dr. Rosso is a member of the Scientific Research Center of the National Research Council (CONICET - Argentina) and Scientific Adviser of the Master on Medical Physics (University of Buenos Aires).

Address for Correspondence: Susana Blanco, Instituto de Cálculo, FCEyN, Universidad de Buenos Aires, Pabellón II, Ciudad Universitaria, 1428 Buenos Aires, Argentina.

References

1. **Gevins AS:** in *Handbook of Electroencephalography and Clinical Neurophysiology, Vol. I: Methods of Analysis of Brain Electrical and Magnetic Signals*, edited by A. Gevins and A. Rémond (Elsevier, Amsterdam, 1987); pp. 31-83.

2. **Dumermuth G, Molinari L:** *in Handbook of Electroencephalography and Clinical Neurophysiology, Vol. I: Methods of Analysis of Brain Electrical and Magnetic Signals*, edited by A. Gevins and A. Rémond (Elsevier, Amsterdam, 1987); pp. 85-130.

3. **Gotman J:** in *Handbook of Electroencephalography and Clinical Neurophysiology, Vol. II: Clinical Applications of Computer Analysis of EEG and Other Neurophysiological Signals*, edited by F.H. Lopes da Silva, Storm van Leeuwen and A. Rémond (Elsevier, Amsterdam, 1986); pp. 685-732.

4. **Lopes da Silva FH:** in *Electroencephalography, Basic Principles, Clinical Applications, and Related Field*, edited by E. Niedermeyer and F.H. Lopes da Silva (Urban and Schwarzenberg, Baltimore, 1987); pp. 871-897.

5. **Gotman J:** in *Current Practice of Clinical Electroencephalography*, edited by D.D. Daly and T.A. Pedley, 2nd ed. (Reven Press Ltd., New York, 1990); pp. 51-83.

6. **Blanco S, García H, Quian Quiroga R, Romanelli L, Rosso OA:** Stationarity of the EEG series. *IEEE Eng. in Med. and Biol.* 14 (1995) 395.

7. **Blanco S, Quian Quiroga R, Rosso OA, Kochen S:** Time-frequency analysis of electroencephalogram series, *Phys. Rev.* E 51, 1995.

8. **Gabor D:** Theory of communication. *J. Inst. Elec. Eng.*, Vol. 93, 429-459, 1946.

9. **Blanco S, D'Attellis, Isaacson S, Rosso OA, Sirne R:** Time-frequency analysis of electroencephalogram series (II): Gabor and Wavelets Transform (to be published) 1995.